Overview of Results from PHOBOS experiment at RHIC

Andrzej Olszewski for the PHOBOS Collaboration:

B B Back†, M D Baker‡, D S Barton‡, R R Betts†+, R Bindel*, A Budzanowski§, W Busza‖, A Carroll‡, J Corbo‡, M P Decowski‖, E Garcia*, N George†, K Gulbrandsen‖, S Gushue‡, C Halliwell+, J Hamblen♯, C Henderson‖, D Hicks‡, D J Hofman+, B Holzman+, R S Hollis+, R Hołyński§, A Iordanova+, E Johnson♯, J L Kane‖, J Katzy‖, N Khan♯, W Kucewicz+, P Kulinich‖, C M Kuo¶, W T Lin¶, S Manly♯, D McLeod+, J Michałowski§, A C Mignerey*, J Mülmenstädt‖, R Nouicer+, A Olszewski‡§, R Pak‡, I C Park♯, H Pernegger‖, M Rafelski‡, M Rbeiz‖, C Reed‖, L P Remsberg‡, M Reuter+, C Roland‖, G Roland‖, L Rosenberg‖, J Sagerer+, P Sarin‖, P Sawicki§, W Skulski♯, S G Steadman‖, P Steinberg‡, G S F Stephans‖, M Stodulski§, A Sukhanov‡, J L Tang¶, R Teng♯, A Trzupek§, C Vale‖, G J van Nieuwenhuizen‖, R Verdier‖, B Wadsworth‖, F L H Wolfs♯, B Wosiek§, K Woźniak‡§, A H Wuosmaa†, B Wysłouch‖

†Argonne National Laboratory, Argonne, USA
‡Brookhaven National Laboratory, Upton, USA
§Institute of Nuclear Physics, Kraków, Poland
‖ Massachusetts Institute of Technology, Cambridge, USA
¶National Central University, Chung-Li, Taiwan
+ University of Illinois at Chicago, Chicago, USA
* University of Maryland, College Park, USA
♯ University of Rochester, Rochester, USA

Abstract. An overview of results for interactions of Au+Au ions at center-of-mass energies of $\sqrt{s_{NN}} = 56$, 130 and 200 GeV obtained by the PHOBOS collaboration at RHIC is given. Measurements of primary charged particle density near mid-rapidity indicate that particle production grows logarithmically with collision energy and faster than linearly with the number of interacting nucleons. Elliptic flow is found to be much stronger at RHIC than at SPS energy. The effect is strongest in peripheral events and decreases for more central collisions and emission angles $|\eta| > 1$. The measured anti-particle to particle ratios of production rates for pions, kaons and protons in central Au+Au interactions at $\sqrt{s_{NN}} = 130$ GeV are compatible with the statistical model of particle production, showing an increasingly barion free region in mid-rapidity with the increase of collision energy.

Submitted to: *J. Phys. G: Nucl. Phys.*

PACS numbers: 25.75.-q

1. Introduction

In the last two years RHIC has delivered collisions of gold ions accelerated to the center-of-mass energies of $\sqrt{s_{NN}} = 56$, 130 and 200 GeV, the highest energies in collision of heavy ions ever produced in accelerators. Collisions of gold ions at such high energies are expected to create nuclear matter at a sufficiently high density and temperature to allow for a phase transition to a new state of matter called Quark Gluon Plasma (QGP). The aim of first measurements performed by the PHOBOS collaboration was to investigate properties of particle production in these new energy regimes and verify if the extreme conditions needed for a phase transition in nuclear matter have actually been achieved.

2. Experimental details

PHOBOS detector is composed of a system of silicon pad detectors designed for detailed measurements of the properties of produced particles, a TOF system for extended particle identification and a triggering system. A detailed description of the experimental apparatus can be found in [1].

Global properties of particle production in an almost full 4π space are measured in a single layer Multiplicity Array composed of Octagon and Ring silicon detectors. Particle identification and momentum measurement can be obtained in a small acceptance, two arm Spectrometer placed in a 2T magnetic field. The Spectrometer arms are built of 16 layers of finely segmented silicon detectors, providing measurements of particle trajectory and energy loss in silicon pads. Particles with emission angles corresponding to $0.5 < \eta < 1.5$ can be reconstructed. Their momenta are calculated from the curvature of the track in the magnetic field. Basing on the averaged energy loss, pions, kaons and protons can be identified for momenta smaller than 1 GeV. Precise position of the interaction point is obtained from tracks of primary particles reconstructed from hits in Spectrometer and a dedicated silicon Vertex detector.

For triggering and centrality determination two arrays of scintillator Paddle counters were used, with additional help from Zero Degree Calorimeters (ZDC). Paddle counters detect produced particles at pseudorapidity $3.0 < |\eta| < 4.5$, while ZDC calorimeters register neutral particles (mostly spectator neutrons) emitted in a very narrow, forward region. A valid collision event is defined by a cut on time differences from pairs of these detectors on both sides of the interaction region, and by requiring a minimum number of Paddle segments to be hit. These cuts remove the background of beam-gas events. The accepted events represent 97% of the inelastic cross section for Au+Au interactions.

Centrality of the collision is determined from the amplitude of the signal in Paddle counters, the quantity which has been verified to grow monotonically with centrality. The full event sample has been divided into centrality bins by taking a defined percentage of events ordered according the decreasing magnitude of the Paddle signal, starting from (0–6%) of the most central events and then moving to more peripheral events. For each of these bins, we have estimated an average number of participating nucleons (N_{part}) using results of Hijing model simulations coupled with full Geant simulations of our detector. See [2] for details.

3. Production of charged particles

Reconstruction of the number of primary particles is done based on hits recorded in Spectrometer, Vertex and Multiplicity Array silicon detectors.

Several methods of reconstruction have been used. In Spectrometer and Vertex detectors simple tracks, called tracklets, constructed of hits in two silicon layers and a vertex point are counted. In single layer detectors of Multiplicity Array, hits in silicon pads are counted directly and then corrected for the probability of several particles crossing the same pad. Detailed description of these reconstruction methods and of corrections applied for secondaries, absorption in detector elements and reconstruction method biases can be found in [3, 4]. Systematic errors have been estimated to range from 4.5% for the tracklet reconstruction in Spectrometer to 10% in hit counting methods. Within these errors all methods of multiplicity reconstruction provide compatible results, therefore we average over them when giving our final numbers.

3.1. Charged particle density at mid-rapidity

Measurement of the charged particle density at mid-rapidity, $dN_{ch}/d\eta|_{|\eta|<1}$, is a good estimate of the energy density produced in nuclear collisions. In PHOBOS we have done this measurement for the 6% most central Au+Au collisions at all three energies delivered by RHIC [4, 5]. The measured density, $dN_{ch}/d\eta|_{|\eta|<1}$ increases from the value of 408 ± 12(stat.)± 30(syst.) at $\sqrt{s_{NN}} = 56$ GeV, to 555 ± 12(stat.)± 35(syst.) at $\sqrt{s_{NN}}$ $= 130$ GeV and to 650 ± 35(syst.) at $\sqrt{s_{NN}} = 200$ GeV.

In order to compare densities measured in interactions of different projectiles we have scaled them by the number of pairs of interacting nucleons. Such comparison is shown in Figure 1, for heavy ion interactions at RHIC, SPS and AGS energies. Over this wide energy range we observe a steady, approximately logarithmic increase of the scaled charged particle density with energy [5]. When compared with densities measured in $\overline{p}p$ collisions, a large difference in particle density per nucleon pair is seen. This indicates that the particle production in mid-rapidity depends not only on the number of participating nucleons but also on the number of nucleon–nucleon collisions.

A more detailed measurement of the dependence of charged particle density at mid-rapidity as a function of centrality has been done by PHOBOS for Au+Au interactions

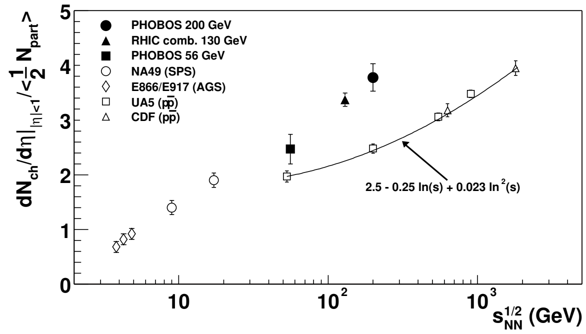

Figure 1. Energy dependence of charged particle density normalized per pair of participating nucleons at mid-rapidity region. Results for central collisions of gold ions obtained at RHIC energies are compared with heavy ion collisions at lower energies and with $\overline{\mathrm{p}}$p data

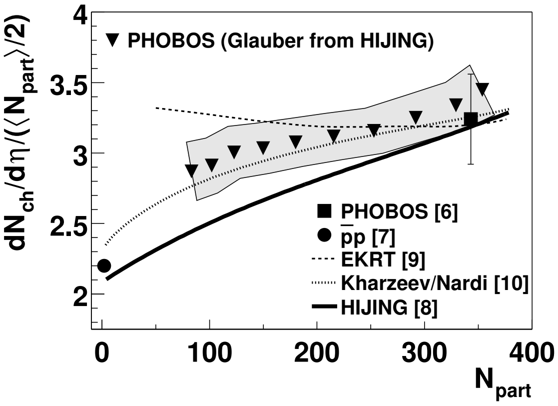

Figure 2. Normalized charged particle density at $|\eta| < 1$ for Au+Au collisions at $\sqrt{s_{NN}}$=130 GeV measured by PHOBOS (solid triangles) and compared with predictions of theoretical models. Early PHOBOS result for 6% central collisions (solid square) and the density in $\overline{\mathrm{p}}$p collisions are also shown.

at $\sqrt{s_{NN}} = 130$ GeV [6]. The result is shown in Figure 2 and compared with predictions from several models. One can see that with increasing number of participating nucleons from 83 to 353 the scaled particle density $dN_{ch}/d\eta|_{|\eta|<1}/\frac{1}{2}N_{part}$ increases from the value of 2.9 to 3.5. This increase is in a disagreement with a simple Wounded Nucleon Model, that predicts a constant number of particles produced per participating nucleon. Other models, shown for comparison in Figure 2, predict either a stronger increase than observed experimentally, as in Hijing [8] or even a decrease in the EKRT saturation model [9]. The two models presented in [10], shown as a dotted line in Figure 2, predict an increase of particle density similar to that observed experimentally. In the first model this is a consequence of increasing contribution from hard parton collisions, while in the second one this is due to the evolution of a gluon structure function with saturation scale. Since both these models give a similar prediction we can not distinguish between the two different scenarios based on the results presented in Figure 2 alone.

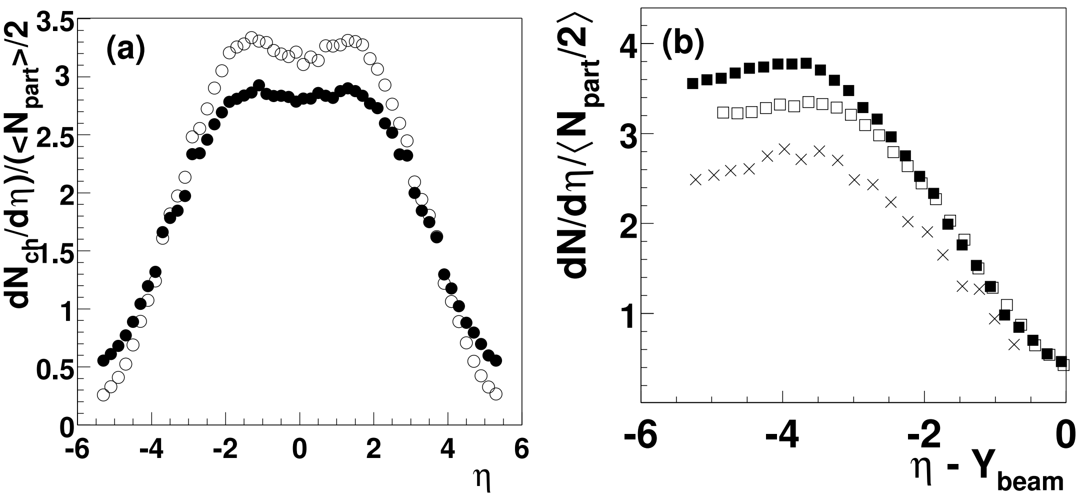

Figure 3. a) Comparison of pseudorapidity distributions of charged particle density normalized per pair of participating nucleons in (35–45%) semiperipheral (full circles) and (0–6%) central (open circles) Au+Au collisions at $\sqrt{s_{NN}}$=130 GeV. b) Comparison of pseudorapidity distributions in the projectile rest frame for normalized charged particle density in Au+Au central collisions at $\sqrt{s_{NN}}$ = 130 GeV (open squares) and 200 GeV (filled squares). Data from UA5 for $\overline{\mathrm{p}}$p collisions are shown by crosses. Systematic errors are not shown.

3.2. Charged particle density distributions in full pseudorapidity range

More details on particle production properties in Au+Au collisions have been obtained after reconstruction of a full angular distribution of charged particles in the range of $|\eta| < 5.4$ at $\sqrt{s_{NN}} = 130$ GeV [3]. A detailed comparison of particle density distributions at the two different centrality bins (0-6% and 35-45%) has been done, scaling them again by the number of pairs of participating nucleons. The results, shown in Figure 3a, confirm the previously observed increase in particle density produced in mid-rapidity with centrality. At larger values of pseudorapidity a decrease of the scaled particle density is observed. This effect can probably be explained by stopping of nucleons participating in the collision, which moves them from regions of higher η to mid-rapidity.

A similar reconstruction of charged particle angular distributions has been done recently also for a sample of 6% most central Au+Au collisions at $\sqrt{s_{NN}}$ = 200 GeV. By comparing angular distributions measured at two highest RHIC energies, $\sqrt{s_{NN}}$ = 130 and 200 GeV we have made an attempt to verify the “limiting fragmentation” hypothesis, which predicts that particle density in the fragmentation region (at large $|\eta|$) should be independent of the collision energy. The two distributions shifted to the projectile rest frame are shown in Figure 3b. It is seen that the two distributions overlap in the fragmentation region, thus we can conclude that the “limiting fragmentation” hypothesis that worked in nucleon–nucleon collisions, is valid also in high energy, heavy ion interactions.

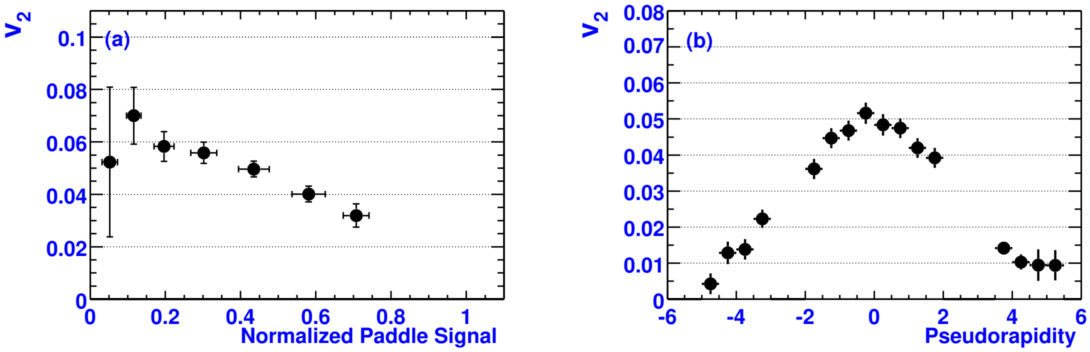

Figure 4. a) Elliptic flow, v_2, measured by PHOBOS in mid-rapidity region $|\eta| < 1$ as a function of centrality, defined here by a normalized signal in Paddle detectors. b) Elliptic flow, v_2, averaged over centrality, as a function of pseudorapidity η. The error bars shown are statistical only. Systematic errors are estimated at constant value of Δv_2=0.007.

4. Flow — the asymmetry in azimuthal distribution of produced particles

The effect of asymmetry in azimuthal angle of produced particles is called flow. It is a reflection of initial state geometrical asymmetry in interactions of two heavy nuclei with impact parameter b≠0. The magnitude of flow is usually measured by Fourier coefficients of the azimuthal particle distribution relative to the event reaction plane, $dN/d(\phi - \Psi_R) = N_0(1 + \sum_i 2v_i \cos[i(\phi - \Psi_R)])$, where Ψ_R is the reaction plane angle. The first component (v_1) is called directed flow and the second one (v_2) elliptic flow. In PHOBOS a measurement of flow has been done using hits in these parts of the Multiplicity Array detector which have a full azimuthal angle coverage. Details of the analysis can be found in [11].

So far in PHOBOS an elliptic flow has been measured in collisions of gold ions at $\sqrt{s_{NN}}$ = 130 GeV. The measurement of elliptic flow in mid-rapidity region as a function of centrality is shown in Figure 4a. A strong increase of flow from the value of 3% in central collisions to 7% in peripheral ones is observed. This behavior is in agreement with the expectations based on the initial state asymmetry arguments, and with predictions of microscopic [12] as well as hydrodynamic models [13]. The measured maximum value of v_2 is much higher than those of 2% measured at AGS and of 3.5% at SPS energies.

Using the wide angle coverage of our Multiplicity Array detector the measurement of elliptic flow has been extended to a full range of psudorapidities, after integrating over all centrality bins in order to increase event statistics. Results obtained for Au+Au events at $\sqrt{s_{NN}} = 130$ GeV are shown in Figure 4b. It is seen that the elliptic flow has a maximum at $\eta = 0$ and then its magnitude decreases quickly at $|\eta| > 1$. This result has been reproduced in calculations of a cascade string model QGSM [12] where it arises as a consequence of secondary interactions of particles in spatially asymmetric system.

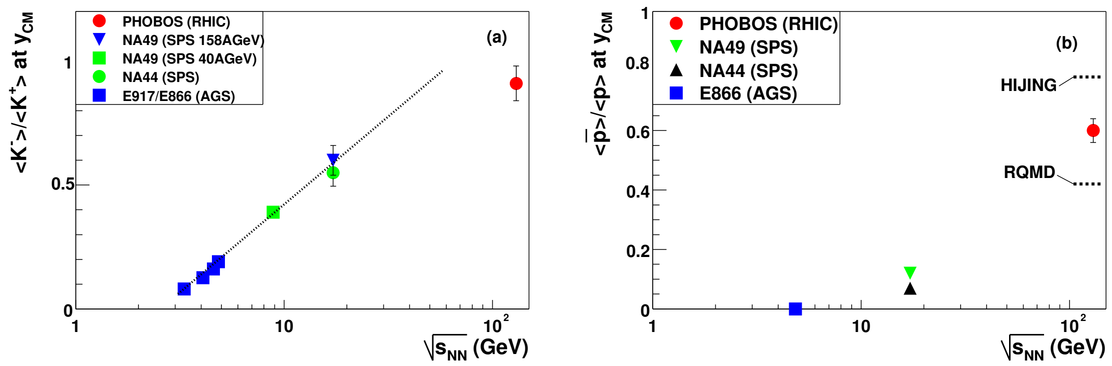

Figure 5. a) Ratio $\langle K^- \rangle / \langle K^+ \rangle$ at mid-rapidity in central collisions of heavy ions as a function of energy. b) Ratio $\langle \overline{p} \rangle / \langle p \rangle$ at mid-rapidity in central collisions of heavy ions as a function of energy. Predictions of Hijing and RQMD models are also shown.

5. Ratios of anti-particle to particle production

A better understanding of processes that occur during nuclear collision can be achieved by studying rates of production of different particle species. They provide information on the thermodynamic state of the interacting system, and on properties of the specific mechanisms of particle creation, absorption and transport.

The measurement of π^-/π^+, K^-/K^+ and $\overline{p}/p$ production ratios at mid-rapidity region have been done in PHOBOS for 12% most central collisions at $\sqrt{s_{NN}} = 130$ GeV, using the Spectrometer detector. The ratios have been corrected for particle decays, secondary interactions and feed-down contribution from strange hadrons. Details can be found in [14]. The following results have been obtained: $\langle \pi^- \rangle / \langle \pi^+ \rangle = 1.00 \pm 0.01(\text{stat.}) \pm 0.02(\text{syst.})$, $\langle K^- \rangle / \langle K^+ \rangle = 0.91 \pm 0.07(\text{stat.}) \pm 0.06(\text{syst.})$, $\langle \overline{p} \rangle / \langle p \rangle = 0.60 \pm 0.04(\text{stat.}) \pm 0.06(\text{syst.})$. A comparison with results obtained at lower energies is shown for kaon and proton ratios in Figure 5a and Figure 5b respectively. It can be seen that the ratio of production of anti-particles to particles increases with increasing energy. Hijing [8] and RQMD [15] models predict well the general trend of the energy dependence but fail to reproduce the exact measured values.

Particle production ratios are also predicted in a statistical model [16]. We have used this model to interpret ratios measured by PHOBOS and we have found that for a fixed freeze-out temperature T=170 MeV, both K^-/K^+ and $\overline{p}/p$ ratios are consistent with a single value of bario-chemical potential $\mu_B = 45 \pm 5$ MeV [14]. This value is much lower than the value of μ_B =240–270 MeV obtained in experiments at SPS energies, indicating that we are getting closer to a barion free state in the central part of the interaction region with the increase of collision energy.

6. Conclusion

The start up of PHOBOS running has been very successful in collecting data from collisions of gold ions accelerated at RHIC to the highest available energies. During this period global properties of particle production in nuclear collisions have been studied and compared with properties of elementary nucleon-nucleon collisions. It has been found that the charged particle density produced in nuclear collisions is growing faster with collision energy than in $\overline{\mathrm{p}}\mathrm{p}$ and that this dependence is logarithmic rather than a power-law like when studied over a wide AGS — RHIC energy range. It has been shown that the particle density increases faster than linearly with increasing number of participating nucleons and that this additional particle production is concentrated in mid-rapidity region.

The measurement of azimuthal asymmetry in particle production has shown a clear elliptic flow signal, in general much stronger than at lower energies, with maximum value in peripheral collisions and in the mid-rapidity region.

In addition to these global features, anti-particle to particle ratios of production rates have been measured. An increase of the ratios with energy, indicates that we are getting very close to barion free state in the mid-rapidity region. These findings tell us that the conditions in collisions at RHIC fulfill minimum requirements for the creation of QGP. PHOBOS experiment is well suited to find signatures of this new state of matter and will be looking for them in the more detailed future studies.

Acknowledgments

This work has been partially supported by US DOE grants DE-AC02-98CH10886, DE-FG02-93-ER-404802, DE-FC02-94ER40818, DE-FG02-94ER40865, DE-FG02-99ER41099, W-31-109-ENG-38, NSF grants 9603486, 9722606 and 0072204. The Polish group has been partially supported by KBN grant 2 PO3B 04916. The NCU group has been partially supported by NSC contract NSC 89-2112-M-008-024.

References

[1] Back B B *et al* 2000 *Nucl. Phys.* **A661** 690
Back B B *et al* 2000 *Nucl. Instrum. Methods* **A447** 257
[2] Katzy J, PHOBOS Collaboration *Proc. Quark Matter 2001* in press
[3] Back B B *et al* 2001 *Phys. Rev. Lett.* **87** 102303
[4] Back B B *et al* 2000 *Phys. Rev. Lett.* **85** 3100
[5] Back B B *et al* 2001 *Preprint nucl-ex/0108009*
[6] Back B B *et al* 2001 *Preprint nucl-ex/0105011*
[7] Abe F *et al* 1990 *Phys. Rev.* **D41** 2330
[8] Wang X N and Gyulassy M 2001 *Phys. Rev. Lett.* **86** 3496
[9] Eskola K J, Kajantie K and Tuominen K 2001 *Phys. Lett.* **B497** 39
[10] Kharzeev D and Nardi M 2001 *Preprint nucl-th/0012025*
[11] Park I C, PHOBOS Collaboration *Proc. Quark Matter 2001* in press
[12] Zabrodin E E *et al* 2001 *Phys. Lett.* **B508** 184
[13] Kolb P F 2001 *Proc. Quark Matter 2001* in press
[14] Back B B *et al* 2001 *Phys. Rev. Lett.* **87** 102301
[15] Sorge H 1995 *Phys. Rev.* **C52** 3291
[16] Redlich K 2001 *Proc. Quark Matter 2001* in press